A Numerical Study on the Improvement of the Thermal Performance of a Solar Chimney Power Plant with Variation in the Absorber

Bambang Arip Dwiyantoro
Department of Mechanical Engineering, Sepuluh Nopember Institute of Technology, Indonesia
bambangads@me.its.ac.id (corresponding author)

Ahmad Fakhruddin
Department of Mechanical Engineering, Sepuluh Nopember Institute of Technology, Indonesia
6007231025@student.its.ac.id

Received: 1 June 2025 | Revised: 12 July 2025 | Accepted: 23 July 2025

Licensed under a CC-BY 4.0 license | Copyright (c) by the authors | *DOI: https://doi.org/10.48084/etasr.12483*

ABSTRACT

Solar Chimney Power Plants (SCPPs) are a promising technology in the advancement of renewable energy systems. Among the various important design parameters, the geometry of the absorber surface plays a pivotal role in determining system performance. This study was conducted to evaluate the impact of the absorber surface geometry and height on the thermal and aerodynamic behavior of SCPPs. Five absorber configurations were investigated: standard, 3-square, 4-square, 5-square, and 6-square arrangements. Additionally, the effect of varying absorber surface heights was examined to identify optimal design parameters. The simulation results demonstrate that the 5-square configuration delivered the highest performance relative to the standard flat-absorber system, particularly at an absorber height of H_o = 7.5 cm, where the maximum airflow velocity reached 24.45 m/s and the power output peaked at 258.38 W. The 3-square configuration also showed notable performance at H_o = 5 cm, generating up to 156.82 W and achieving the lowest internal atmospheric pressure, indicative of improved convective flow. Overall, the findings emphasize the substantial influence of absorber surface design on SCPP efficiency, confirming that multi-square absorber configurations can significantly enhance power generation through improved thermal and fluid dynamic behavior.

Keywords-solar chimney; modified absorber; power generation; natural convection

I. INTRODUCTION

A Solar Chimney Power Plant (SCPP) is a promising renewable energy technology that harnesses solar radiation to drive airflow through a tall chimney, thereby generating electricity via a turbine system [1]. The basic operating principle involves heating air beneath a transparent collector, reducing its density, and causing it to rise through a vertical chimney. This upward airflow drives centrally located turbines, converting thermal energy into mechanical energy and subsequently into electrical energy. The SCPP system is particularly appealing due to its utilization of abundant solar resources, structurally simple design, and extremely low carbon emissions, offering a sustainable alternative to conventional fossil fuel-based energy systems [2-3]. The first SCPP prototype was constructed in Manzanares, Spain, and successfully generated 50 kW of electrical power [4]. Since then, numerous studies have been conducted to assess and optimize SCPP performance. Authors in [5] investigated the optimal dimensions of the SCPP, finding that chimney height, tower diameter, and collector inlet elevation significantly influence system performance. Authors in [6, 7] reported that increasing the collector and chimney radius/height directly enhances airflow velocity and, consequently, energy output. Authors in [8-10] further confirmed that the power output of an SCPP increases with the diameter of the collector and the height of the chimney. Additionally, the effects of collector and chimney geometric parameters have been extensively examined through numerical simulations in [11, 12].

The relatively low thermal efficiency and power output of an SCPP highlight the need for further design optimization. One of the key components influencing system performance is the absorber surface located beneath the collector. The geometry of this surface significantly affects solar energy absorption, heat transfer processes, and airflow behavior within the system. The shape of the absorber surface can play a critical role in determining the overall efficiency of the solar chimney. Authors in [13] conducted a numerical investigation on the impact of various absorber surface geometries on the power output of the solar chimney. The studied configurations included right-angled triangles, equilateral triangles, squares, and semi-circular shapes. Among these, the square-shaped absorber surface

demonstrated a power output enhancement of up to 67.4% compared to a flat surface. These findings provide valuable insights for the development of more efficient solar chimney systems. In [14], the authors modified the absorber surface into a triangular wave-like profile, varying the number of triangular elements (n = 1, 3, 5, and 7) and the absorber height between 0.25 and 1.25. Their results showed that a wavy absorber surface could increase the power output by as much as 58.61% relative to a flat design.

Another critical factor in SCPP design is the chimney divergence angle. Different chimney configurations, such as convergent, divergent, sudden contraction, sudden expansion, and inclined ground absorbers have been found to influence the performance of the system. A divergent chimney design demonstrated a significant improvement in power output when compared to a standard cylindrical chimney [15]. Specifically, a divergent chimney with an inclination angle of 0.6º was shown to enhance power generation by up to 60% [16]. Appropriate divergence improves airflow velocity and pressure drop across the turbine, thereby increasing power generation.

Although the above-mentioned studies have provided substantial insights, most of them evaluated absorber surface geometry and chimney divergence angle independently. The interactive influence of these two critical parameters on system performance has not been extensively investigated, representing a significant gap in the current body of knowledge. Furthermore, the existing studies have not addressed the performance implications of multiple square-based absorber configurations in combination with a fixed divergent chimney, particularly under uniform simulation conditions. This study seeks to bridge this gap by numerically investigating the impact of various absorber surface geometries in conjunction with a fixed chimney divergence angle on the thermal and aerodynamic performance of an SCPP. The absorber is modeled using multiple square-based configurations comprising 3-square, 4-square, 5-square, and 6-square arrangements at different surface heights. Meanwhile, the chimney features a constant divergence angle of 0.6°. Simulations were conducted under standardized pressure inlet conditions, with system performance assessed by comparing thermal efficiency and power output against a reference model derived from the small-scale prototype developed in [5].

The novelty of this study lies in its integrative approach, which systematically combines two influential yet often separately analyzed design parameters. By doing so, it not only complements prior findings but also contributes new insights to the existing literature, particularly regarding design strategies that enhance airflow behavior, heat transfer, and energy conversion within SCPPs. The outcomes of this research are expected to improve the technical performance, economic viability, and environmental sustainability of SCPPs, thereby supporting broader global efforts toward renewable energy integration.

II. DATA AND METHODOLOGY

In this system, the SCPP harnesses solar radiation to generate electricity. Ambient air enters through the collector inlet (A) and is heated by solar energy, as the collector is constructed from transparent polyethylene film that permits solar radiation to pass through. The increase in air temperature within the collector reduces its density, causing the heated air to rise through the chimney (B) and eventually be discharged back into the atmosphere. Before entering the chimney, the air passes through a turbine positioned between the collector and the chimney. This turbine, connected to an electrical generator, converts the mechanical energy of the moving air into electrical energy. The operational principle of the solar chimney power generation system is illustrated in Figure 1.

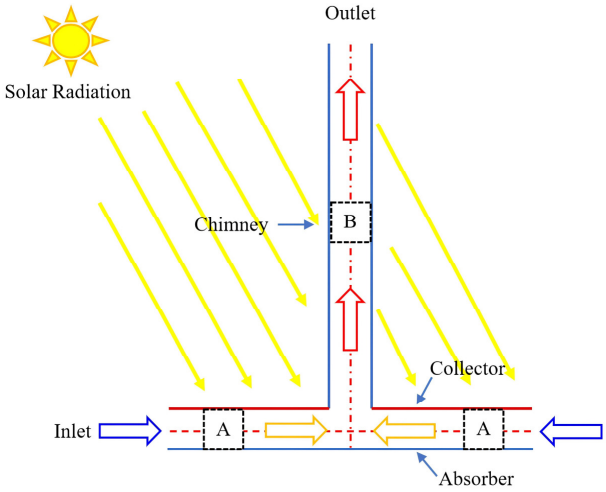

Fig. 1. The working mechanism of the SCPP.

The SCPP comprises several key components, including the absorber surface, the collector, and the chimney. The rise in air temperature is primarily facilitated by the collector, which absorbs incoming solar radiation and transfers the thermal energy to the working fluid. When solar radiation reaches the ground surface, it is reflected upward toward the inner surfaces of the collector, enhancing heat transfer. Polyethylene film is commonly employed as the collector material due to its relatively high efficiency, achieving thermal efficiencies of up to 70% [17], making it preferable over alternative materials.

A. *Physical Model*

The physical domain of the Solar Chimney Power Plant (SCPP) is depicted in Figure 2. The geometric configuration was developed based on the Manzanares prototype [4], employing a fixed divergent chimney angle of 0.6°. The primary geometric parameters utilized in the model are summarized in Table I. Figure 3(a) illustrates the baseline configuration, featuring a conventional horizontal flat ground absorber plate. To enhance the system's thermal performance, the absorber surface was modified into a square wavy bottom wall with varying geometries: 3-square, 4-square, 5-square, and 6-square arrangements. A detailed schematic of each simulation configuration is presented in Figure 3(b). These geometric modifications were introduced to evaluate the effects of absorber surface shape on thermal performance and airflow characteristics within the solar chimney system. By altering only the absorber surface geometry while keeping the chimney angle

and boundary conditions constant, the study seeks to isolate and assess the impact of surface divergence on velocity fields, temperature distribution, and pressure gradients. This methodological approach enables a systematic analysis of how geometric alterations influence the overall efficiency of solar chimney power generation. Furthermore, the influence of the absorber surface height was investigated by testing three different square wave amplitudes, H_0 = 2.5 cm, 5 cm, and 7.5 cm. The material properties employed in the model are detailed in Table II.

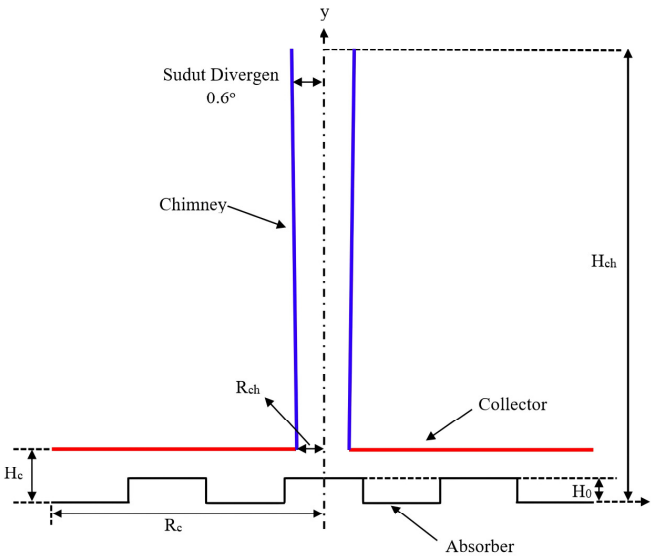

Fig. 2. The pysical model of the SCPP.

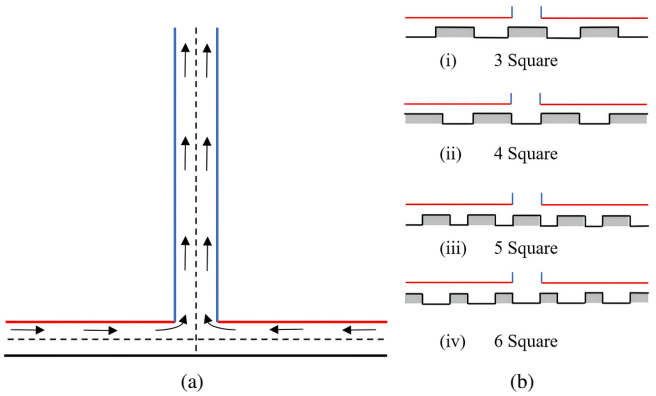

Fig. 3. Schematic diagram of an SCPP model: (a) SCPP with standard flat ground absorber, (b) modified square absorber.

TABLE I. GEOMETRIC PARAMETER OF A SMALL-SCALE SCPP

Geometric Parameter	Dimension (cm)
Collector radius (R_c)	150
Collector height (H_c)	10
Chimney height from collector surface (H_{ch})	300
Collector radius (R_{ch})	10
Variation of square absorber height (H_0)	2.5, 5, and 7.5

TABLE II. MATERIAL PROPERTIES

Material	**ρ (kg/m³)**	**Cp (J/kg·K)**	**λ (W m^{-1} K^{-1})**	**Thickness (mm)**
Fluid (Air)	1.22	1006.43	0.0242	-
Collector (Polyethylene- film)	920	720	0.33	3
Absorber (Black-rubber)	1260	1360	0.1	4
Chimney (PVC- pipe)	1630	1300	0.13	4

TABLE III. BOUNDARY CONDITIONS

Zone	**Type**	**Property**	**Value**
Inlet	Pressure Inlet	Pressure (Pa)	101325
		Temperature T_0 (K)	305.5
Outlet	Pressure Outlet	Pressure (Pa)	101325
Absorber	Opaque Wall (Mixed)	Heat transfer coefficient h (W/m^{2}K)	5
		Temperature T (K)	305.5
Collector	Semi-Transparent Wall (Mixed)	Heat transfer coefficient h (W/m^{2}K)	5
		Temperature T (K)	305.5
Chimney	Opaque Wall (Heat Flux)	Heat Flux Q (W/m^2)	0

B. Numerical Procedure

Figure 4 illustrates the meshing grid model utilized for the SCPP simulation. A structured quadrilateral mesh was employed to discretize the computational domain. Multiple mesh densities were tested to ensure solution accuracy, with the final mesh consisting of 740,437 cells, which demonstrated mesh independence as further refinement produced negligible changes in the results. This mesh configuration was therefore adopted for all simulation cases. The boundary conditions applied to the computational domain are summarized in Table III. A pressure inlet condition is assigned at the domain's inlet, while a pressure outlet condition is imposed at the outlet. The chimney wall is modeled as adiabatic and opaque. In contrast, the collector and absorber surfaces are defined as semi-transparent and opaque, respectively, with mixed thermal boundary conditions applied to both surfaces. The steady-state airflow and natural convection phenomena within the SCPP were simulated using ANSYS Fluent, which solves the governing equations based on the finite volume method. Turbulence effects were modeled using the standard k–ε turbulence model. The pressure–velocity coupling was resolved using the SIMPLE (Semi-Implicit Method for Pressure Linked Equations) algorithm. Convective terms were discretized using a second-order upwind scheme to ensure higher numerical accuracy [18]. A convergence criterion of 10^{-6} was set for all residuals to minimize numerical error. It is important to note that thermal radiation was not considered in this simulation, which may affect the accuracy of heat transfer prediction, especially in regions where radiative effects are significant. The meshing strategy plays a crucial role in achieving reliable and accurate simulation results.

C. Estimation of Performance Parameters

The performance of the SCPP can be assessed through the power output of the system, which corresponds to the kinematic power generated by the chimney and is mathematically represented as follows [19–20].

The potential power output is defined as [19-20]:

$$P_{op} = \dot{m}\, c_p\, \Delta T\, \eta_{ch} \quad (1)$$

where $\dot{m}$ is the mass flow rate, c_p is the specific heat capacity, ΔT is the temperature difference between the collector inlet and the collector outlet, and η_{ch} is the chimney efficiency, as follows:

$$\dot{m} = \rho\, V_{ch}\, A_{ch} \quad (2)$$

$$\eta_{ch} = \frac{g\, H_{ch}}{c_p\, T_0} \quad (3)$$

where g, ρ, A_{ch}, and V_{ch} are the gravitational acceleration, density, the chimney entrance area, and the airflow velocity at the chimney bottom.

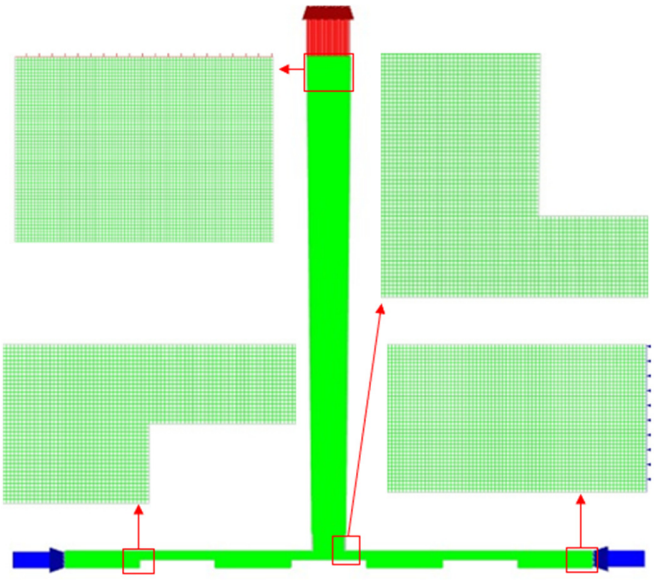

Fig. 4. Meshing grid for the SCPP.

III. RESULTS AND DISCUSSION

A. *Effect of the Absorbent Surface Shape on SCPP Performance*

Five different absorber surface geometries were explored, i.e. a standard flat surface and modified square absorbers with undulation numbers n = 3, 4, 5, 6, to assess their impact on the performance of SCPP. To maintain consistency in the geometric comparison, the absorber height (H_0) was uniformly set to 5 cm for all configurations.

1) Velocity Field

Figure 5 illustrates the velocity field magnitude within the SCPP for each analyzed configuration. The airflow begins with relatively low velocity at the collector entrance and gradually accelerates along the collector. Simulation results confirm that the air velocity consistently increases from the collector inlet toward the base of the chimney. Notably, in all scenarios, a pronounced rise in velocity was observed at the bottom of the chimney, indicating this location is optimal for turbine installation. The comparative analysis reveals that modifying the absorber surface significantly influences airflow velocity, although the velocity magnitude and distribution differ among the various cases. In particular, variations are evident not only in the intensity of peak velocities but also in the shape and extent of the high-velocity zones. Among all configurations, the absorber design with three undulations yielded the highest airflow velocity. Figure 9 confirms these findings. This can be attributed to its geometry, which narrows the airflow path and thereby intensifies acceleration. These results underscore the critical impact of absorber surface geometry on shaping airflow dynamics and enhancing the overall energy conversion efficiency of the system.

2) Thermal Field

Figure 6 presents the temperature distribution for different absorber surface configurations. The simulation results indicate a consistent thermal behavior across all designs: air temperature near the collector inlet remains close to ambient levels and gradually rises toward the center of the collector, primarily due to the greenhouse effect. This temperature increase is largely driven by the absorber material, which possesses high solar absorptivity and low reflectivity and transmissivity, enabling it to retain the majority of incident solar radiation. As a result, the ground surface exhibits the highest temperature among all components of the system. In contrast, the collector wall constructed from transparent polyethylene film shows lower average temperatures due to its low thermal conductivity and the influence of convective cooling occurring on both its inner and outer surfaces. Although the overall temperature distribution trend remains similar among all configurations, variations in maximum temperatures are evident. The highest temperature was observed in the standard flat surface configuration, suggesting that thermal accumulation is more significant when the airflow velocity is lower. These observations are consistent with the findings reported in [15]. Additionally, the vertical temperature profiles along the chimney axis, depicted in Figure 10, further validate this pattern across all tested designs.

3) Pressure Field

The pressure distribution within the SCPP system offers valuable insights into the pressure differential between the collector inlet and the chimney outlet, a key factor influencing the chimney's draft effect. Figure 7 displays the atmospheric pressure contours for the various absorber surface configurations examined. The static pressure patterns across the different cases exhibit similar overall trends. As air enters the collector at atmospheric pressure, the pressure gradually decreases along the collector length, reaching its lowest point at the base of the chimney. From there, it steadily rises until returning to atmospheric pressure at the chimney outlet.

This pressure drop is primarily driven by thermal buoyancy, which generates a strong draft that propels airflow through the system. Among all configurations, the 3-square absorber design exhibited the lowest pressure value, indicating superior suction performance. These findings underscore the significant influence of absorber geometry on internal pressure behavior and the overall efficiency of the system.

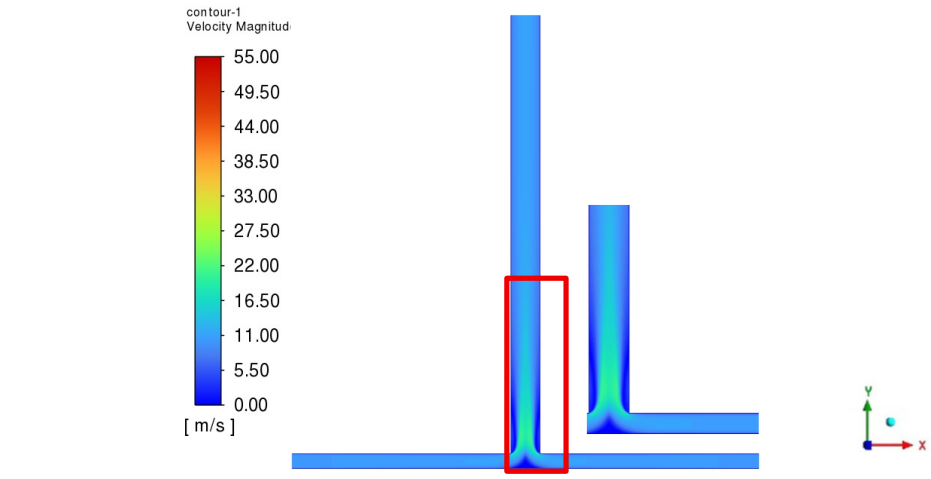

(a) Standard Chimney

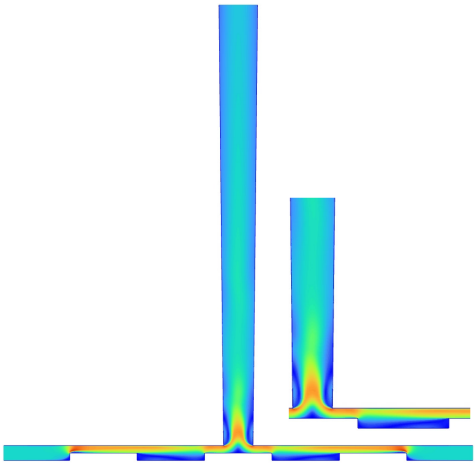

(b) 3 square

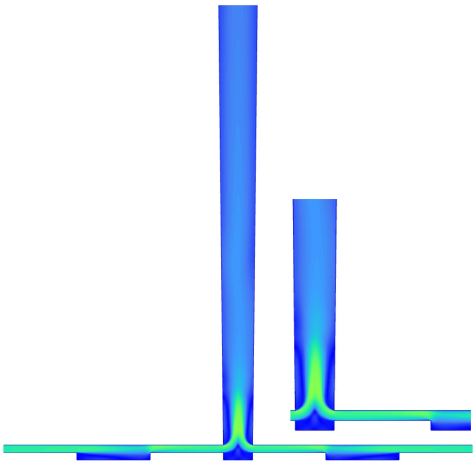

(c) 4 square

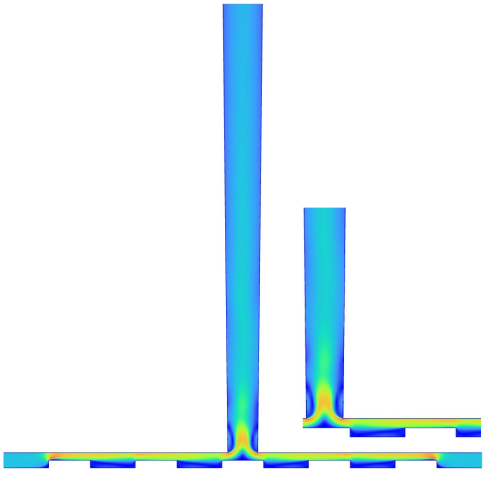

(d) 5 square

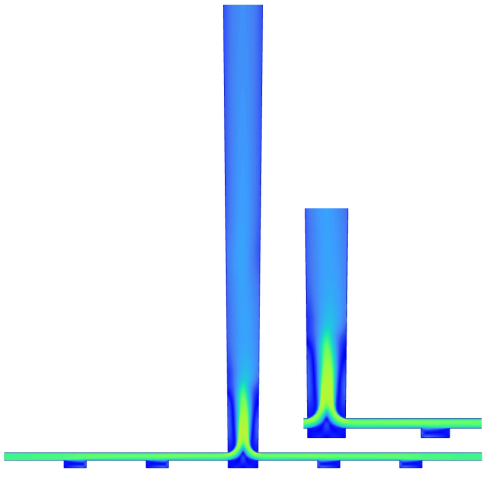

(e) 6 square

Fig. 5. Distribution of the velocity magnitude for different absorber surfaces of SCPP design with H_0 = 5 cm.

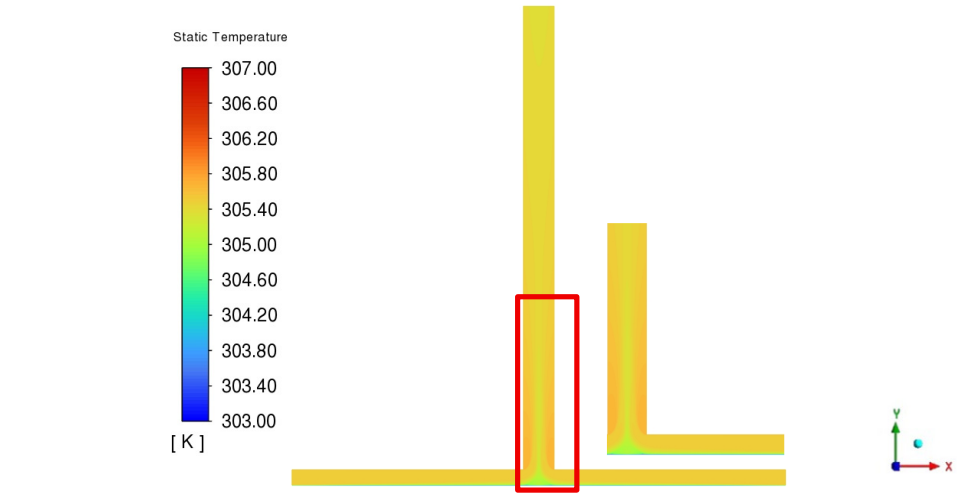

(a) Standard Chimney

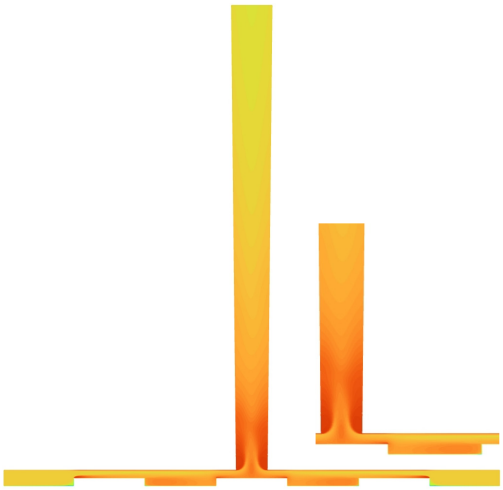

(b) 3 square

(c) 4 square

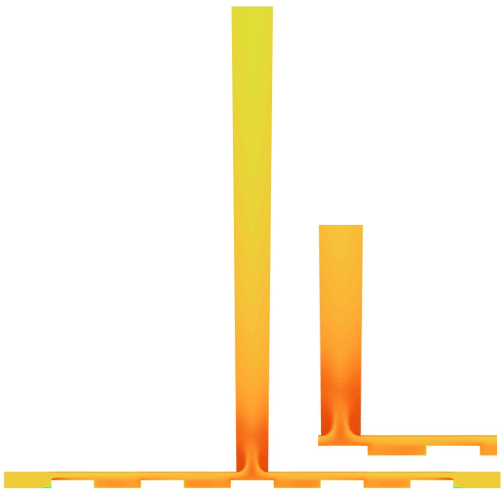

(d) 5 square

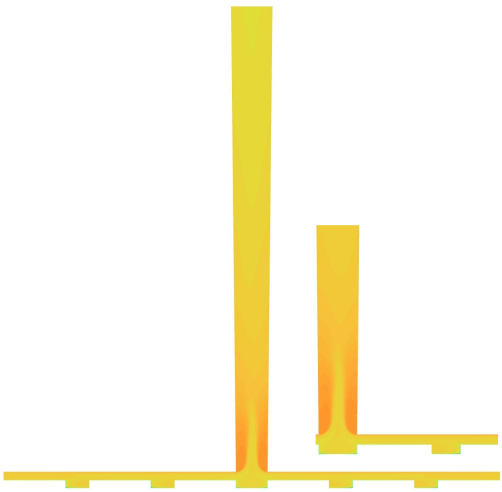

(e) 6 square

Fig. 6. Distribution of the temperature for different absorber surfaces of the SCPP design with H_0 = 5 cm.

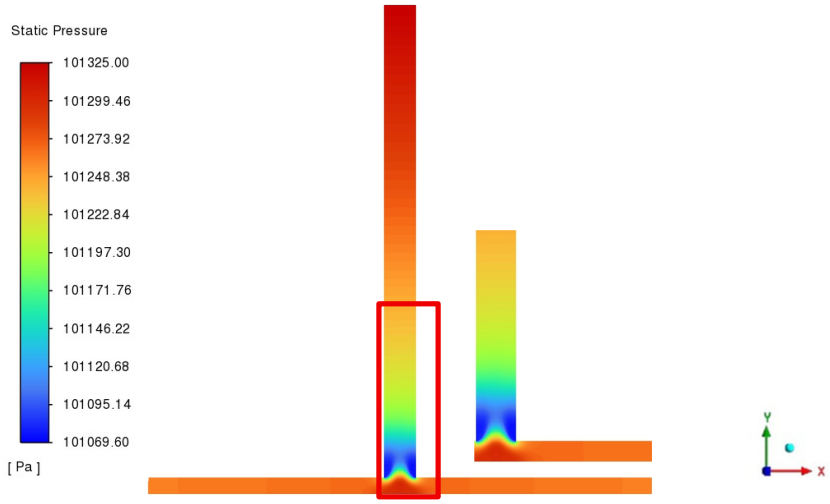

(a) Standard Chimney

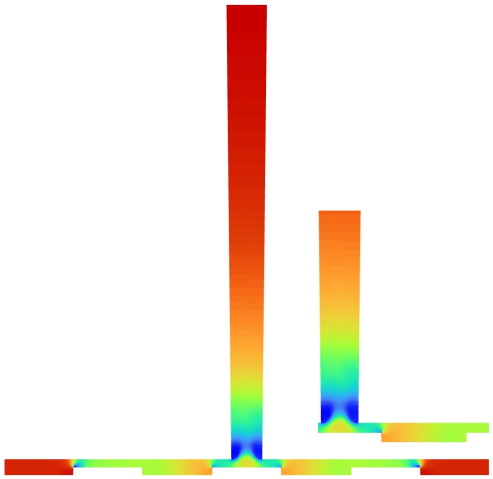

(b) 3 square

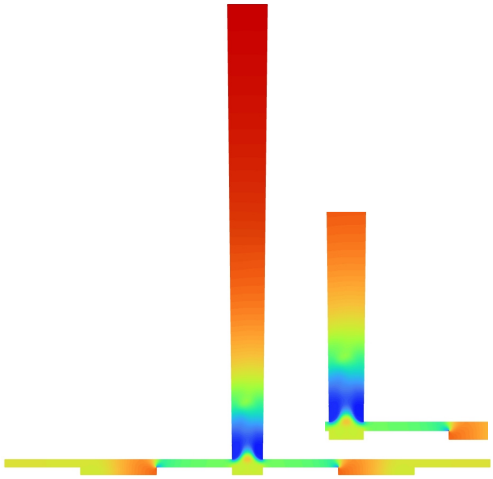

(c) 4 square

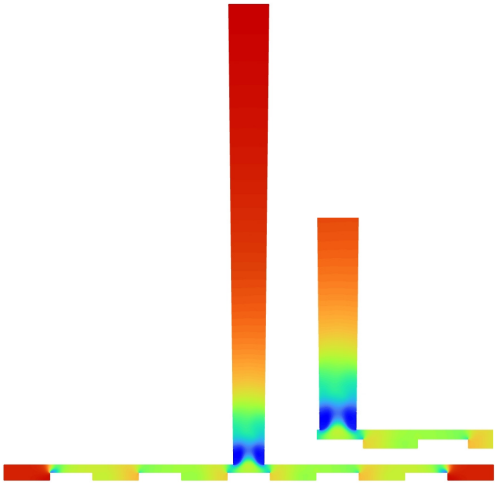

(d) 5 square

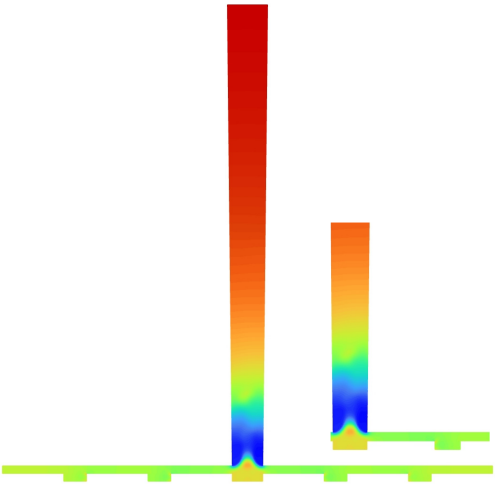

(e) 6 square

Fig. 7. Distribution of the pressure for different absorber surfaces of the SCPP design with H_0 = 5 cm.

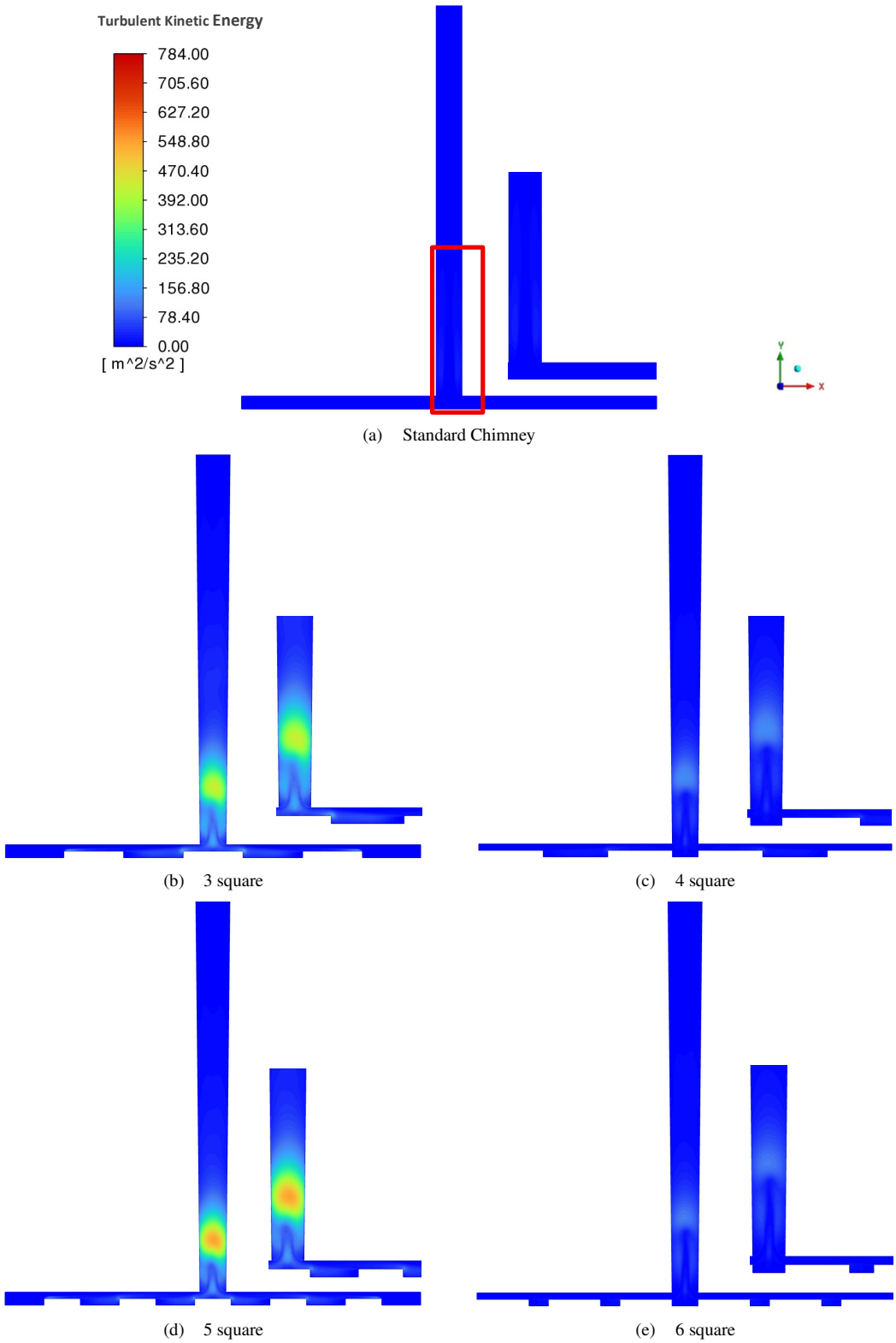

(a) Standard Chimney

(b) 3 square

(c) 4 square

(d) 5 square

(e) 6 square

Fig. 8. Distribution of the turbulence kinetic energy for different absorber surfaces of the SCPP design with $H_0 = 5$.

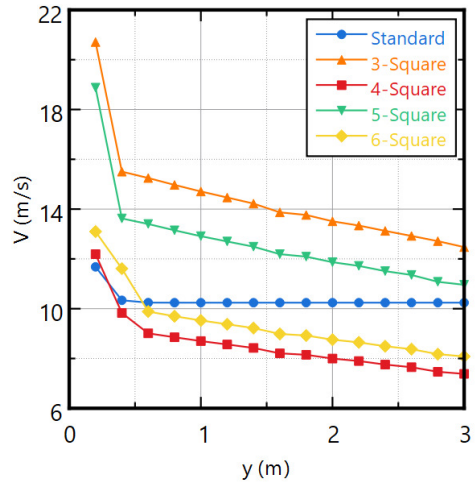

Fig. 9. Maximum velocity profile along the chimney axis.

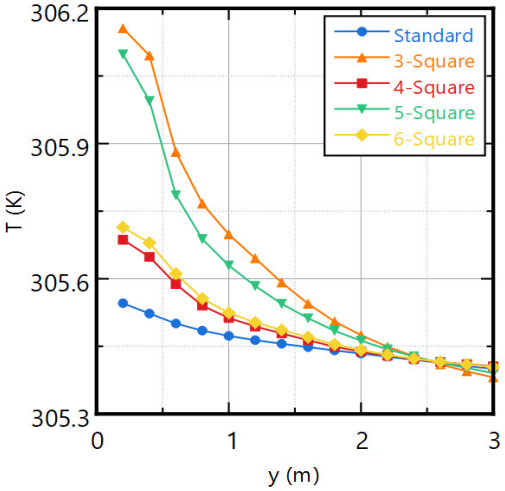

Fig. 10. Profile of the temperature along the chimney axis.

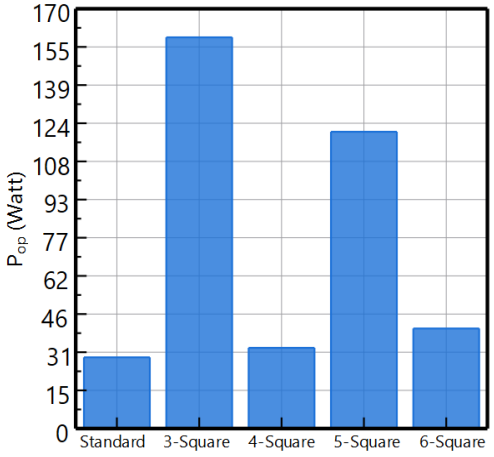

Fig. 11. Potential power output under the condition H_0 = 5 cm.

4) Turbulent Kinetic Energy Field

Figure 8 illustrates the distribution of the Turbulent Kinetic Energy (TKE) for all the absorber surface configurations. The simulation results demonstrate that turbulence intensity within the collector remains notably low across all designs, indicative of predominantly laminar flow conditions. This behavior is primarily attributed to the compact scale of the SCPP system. A marked increase in TKE is consistently observed at the chimney inlet, resulting from abrupt geometric transitions and the acceleration of heated air as it ascends. The absorber surface geometry significantly influences the peak TKE values. Among the evaluated configurations, the 3-square design exhibits the highest TKE, while the traditional flat surface shows the lowest. These findings underscore the role of absorber geometry in modulating not only temperature and velocity distributions but also turbulence intensity, particularly within the transition region between the collector and chimney. Such insights are crucial for optimizing SCPP performance through geometric modifications.

The interaction between turbulence and buoyancy plays a central role in determining the overall performance of solar chimney systems. In buoyancy-driven flows, the upward motion of the air is primarily caused by density differences due to heating. However, as the temperature gradient increases, especially near the heated absorber surface, so does the tendency for flow instabilities, which leads to the onset of turbulence. Turbulence affects the system in two contrasting ways. Moderate turbulence enhances convective heat transfer from the absorber surface to the airflow, increasing the thermal energy input to the system. This intensifies buoyant forces and can accelerate the flow within the collector and chimney. On the other hand, excessive turbulence introduces chaotic eddies and mixing, which dissipate kinetic energy and reduce the efficiency of converting thermal energy into mechanical power.

5) Generated Power

Figure 11 illustrates the power output corresponding to different absorber surface geometries. The results indicate that altering the shape of the absorber surface leads to a significant enhancement in power generation. This improvement is primarily attributed to the increased global efficiency, consistent with the findings reported in [21]. The configurations proposed in this study demonstrate superior performance compared to the conventional SCPP design. A detailed comparison of the power output for various absorber surface geometries is presented in Table IV. Notably, the 3-square absorber configuration resulted in a 449% improvement in chimney performance, while the 5-square absorber configuration achieved a remarkable increase of 317%.

TABLE IV. INCREASE IN THE POWER OUTPUT COMPARED TO STANDARD CHIMNEY FOR DIFFERENT CASES (H_0 = 5 cm)

Design	P_{op} (Watt)	Improvement
Standard	28.84	-
3-Square	158.43	449%
4-Square	32.69	13%
5-Square	120.19	317%
6-Square	40.52	40%

B. Effect of Absorption Variation H_0 on the Performance

This section examines the influence of absorber height on airflow characteristics within the SCPP. Three absorber heights were analyzed across all configurations: H_0 = 2.5 cm, 5 cm, and 7.5 cm. Figure 12 presents the variations in maximum velocity and temperature corresponding to each height for the proposed models. The results demonstrate that absorber height significantly affects both the airflow velocity and temperature distribution within the system. An increase in H_0 leads to a rise in maximum velocity, primarily due to a reduction in flow resistance at the chimney inlet and enhanced buoyancy forces. For instance, a maximum velocity of 24.45 m/s was recorded at H_0 = 7.5 cm with the 5-square absorber surface, representing an increase of 109% compared to the standard SCPP, which achieved only 11.68 m/s. Similarly, at H_0 = 5 cm with the 3-square absorber, the maximum velocity also reached 20.71 m/s again, a 77% improvement over the standard design. These results reinforce the effectiveness of both 3-square and 5-square absorber configurations.

(a)

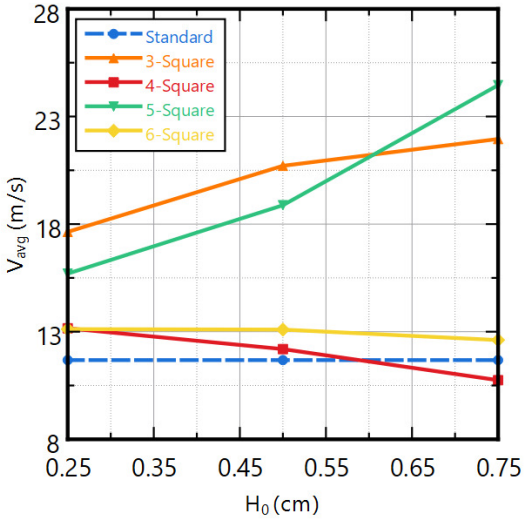

(b)

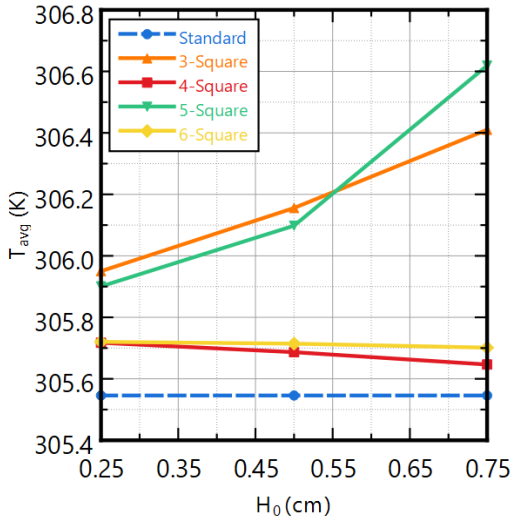

Fig. 12. Maximum of (a) velocity (a) and (b) temperature (b) in the chimney for varying H_0.

Regarding the temperature field, a comparable trend was observed, with the temperature rising in conjunction with absorber height. The highest temperature increase recorded was 0.35% relative to the standard SCPP configuration.

Figure 13 illustrates the power output of the SCPP for various absorber heights. The results reveal a clear dependence of the power output on the absorber height, with a consistent increase in energy generation as H_0 increases. The most notable enhancement is observed for the 5-square absorber surface at H_0 = 7.5 cm, where the power output reaches 258.38 W, representing a remarkable 769% improvement over the standard SCPP. This result can be meaningfully compared to the findings of the authors in [13], who examined several basic absorber geometries such as right-angled triangles, equilateral triangles, squares, and semi-circular shapes and concluded that the square shape offered the highest improvement in power output (up to 67.4%) over a flat design. Our study extends this insight by demonstrating that arranging multiple square absorbers in series (e.g. 3-square to 6-square) can provide even greater efficiency gains, particularly in the 5-square configuration. Additionally, authors in [14] explored triangular wave-shaped absorber profiles and showed that varying the number of triangular elements (n = 1, 3, 5, and 7) and their height led to a maximum power output improvement of up to 58.61%. In comparison, our best-performing case (5-square at H_0 = 7.5 cm) achieved a peak power output of 258.38 W, exceeding the improvements reported in [14] under similar thermal driving conditions. This suggests that modular square arrangements offer a promising alternative to more complex wave-based geometries, with advantages in both performance and structural simplicity. Moreover, unlike both prior studies, which focused solely on absorber shape, our work incorporates the effect of a fixed chimney divergence angle (0.6°), offering a more holistic understanding of how combined design variables affect system performance. This integrative approach represents a novel contribution to SCPP research and provides a basis for future experimental or prototype-based validation.

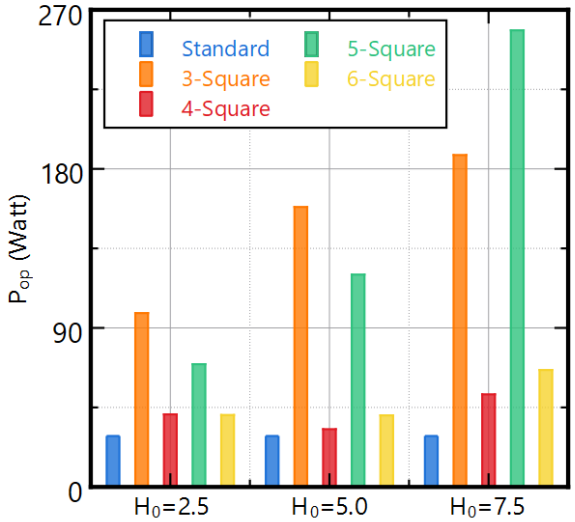

Fig. 13. Output power on the chimney for different H_0

TABLE V. OUTPUT POWER IMPROVEMENT COMPARED TO THE STANDARD CHIMNEY

Design	Improvement		
	H_0 = 2.5 cm	H_0 = 5 cm	H_0 = 7.5 cm
3-Square	241%	449%	551%
4-Square	42%	13%	82%
5-Square	141%	317%	769%
6-Square	41%	40%	129%

This substantial increase can be attributed to the combined effects of the modified absorber geometry and elevated inlet height, which together enhance airflow velocity and pressure differential, thereby boosting the kinetic energy within the chimney. These findings underscore the critical influence of system geometry on the overall efficiency and performance of SCPPs. Further details regarding performance improvements across all configurations are provided in Table V.

The 3-square absorber configuration demonstrates superior performance in terms of airflow velocity and pressure due to its increased exposed surface area and geometric segmentation, which promote enhanced heat absorption and stronger localized buoyancy-driven flow. The discrete square patterns generate intensified thermal gradients across each module, facilitating rapid air expansion and accelerated upward movement. This leads to higher velocities at the chimney base and increased static pressure within the collector. However, as the absorber height increases, the advantage in power output begins to decline. The extended vertical surface results in longer airflow paths, which exacerbate viscous losses due to wall friction and increase pressure drop across the system. Additionally, the segmented geometry of the squares can induce complex flow separations and vortices, particularly at greater heights, which contribute to higher turbulence intensity. While some turbulence aids heat transfer, excessive turbulence dissipates kinetic energy, reducing the amount of energy converted into useful power. As a result, the aerodynamic inefficiencies and increased resistance in tall absorber configurations counteract the benefits of higher flow velocities, leading to a relative decline in net power output.

IV. CONCLUSION

To enable a thorough assessment of a Solar Chimney Power Plant (SCPP) performance, a comparative analysis was performed in this paper, across five absorber surface configurations: standard, 3-square, 4-square, 5-square, and 6-square. Numerical simulation results indicate that the 5-square configuration exhibited the most favorable performance, particularly at an absorber height of H_0 = 7.5 cm, yielding the highest recorded airflow velocity of 24.45 m/s and a peak power output of 258.38 W. The 3-square configuration also demonstrated notable efficiency, especially at H_0 = 5 cm, with a maximum power output of 156.82 W and the lowest recorded atmospheric pressure, suggesting enhanced convective effectiveness. The divergent 4-square and 6-square configurations produced moderate and relatively stable outcomes, yet remained less efficient overall compared to the 3-square and 5-square alternatives. Conversely, the standard configuration consistently resulted in the lowest values for all performance metrics, including airflow velocity, temperature, pressure, and power generation, thereby identifying it as the least efficient design. These results underscore the significant impact of absorber surface geometry on both the thermal and aerodynamic performance of SCPP systems, with multi-square arrangements offering substantial gains in system efficiency.

The novelty of this study lies in its integrative evaluation of multiple square-based absorber geometries in combination with a fixed chimney divergence angle. This approach has not been comprehensively explored in previous research. Unlike earlier works that focused on individual design parameters, this study presents a holistic framework to assess their combined influence on airflow dynamics and energy conversion efficiency. The identification of optimal geometries, such as the 5-square and 3-square arrangements, offers a practical reference for enhancing system design, especially for future applications in renewable energy infrastructure.

REFERENCES

[1] E. Cuce, P. M. Cuce, S. Carlucci, H. Sen, K. Sudhakar, Md. Hasanuzzaman, and R. Daneshazarian, "Solar Chimney Power Plants: A Review of the Concepts, Designs and Performances," *Sustainability*, vol. 14, no. 3, 2022, Art. no. 1450, https://doi.org/10.3390/su14031450.

[2] M. Tawalbeh, S. Mohammed, A. Alnaqbi, S. Alshehhi, and A. Al-Othman, "Analysis for hybrid photovoltaic/solar chimney seawater desalination plant: A CFD simulation in Sharjah, United Arab Emirates," *Renewable Energy*, vol. 202, pp. 667-685, Jan. 2023, https://doi.org/10.1016/j.renene.2022.11.106.

[3] S. Ali and B. Djaouida, "Investigating the feasibility of integrating vegetation into solar chimney power plants in the Tamanrasset Region," *Engineering, Technology & Applied Science Research*, vol. 14, no. 3, pp. 14719-14724, Jun. 2024, https://doi.org/10.48084/etasr.7506.

[4] W. Haaf, K. Friedrich, G. Mayr, and J. Schlaich, "Solar chimneys part I: principle and construction of the pilot plant in Manzanares," *International Journal of Solar Energy*, vol. 2, no. 1, pp. 3–20, 1983, https://doi.org/10.1080/01425918308909911.

[5] M. Ghalamchi, A. Kasaeian, M. Ghalamchi, and A. H. Mirzahosseini, "An experimental study on the thermal performance of a solar chimney with different dimensional parameters," *Renewable Energy*, vol. 91, pp. 477-483, Jun. 2016, https://doi.org/10.1016/j.renene.2016.01.091.

[6] R. Mehdipour, S. Golzardi, and Z. Baniamerian, "Experimental justification of poor thermal and flow performance of solar chimney by an innovative indoor experimental setup," *Renewable Energy*, vol. 157, pp. 1089–1101, Sep. 2020, https://doi.org/10.1016/j.renene.2020.04.158.

[7] B. Ghernaout, S. Bouabdallah, M. E. H. Attia, M. Arıcı, and Z. Driss, "Parametric study of the airflow structure in a solar chimney," *International Journal of Heat and Technology*, vol. 38, no. 2, pp. 285–292, 2020, https://doi.org/10.18280/ijht.380202.

[8] P. Belkhode, C. Sakhale, and A. Bejalwar, "Evaluation of the experimental data to determine the performance of a solar chimney power plant," *Materials Today: Proceedings*, vol. 27, no. 1, pp. 102–106, Jan. 2020, https://doi.org/10.1016/j.matpr.2019.09.006.

[9] A. Ayadi, A. Bouabidi, Z. Driss, and M. S. Abid, "Experimental and numerical analysis of the collector roof height effect on the solar chimney performance," *Renewable Energy*, vol. 115, pp. 649–662, Jan. 2018, https://doi.org/10.1016/j.renene.2017.08.099.

[10] A. Lahcene, A. Y. Benazza, and M. Benguediab, "The effect of geometric parameters on the performance of solar chimney: A numerical and experimental study," *Engineering, Technology & Applied Science Research*, vol. 10, no. 6, pp. 6456-6461, Dec. 2020, https://doi.org/10.48084/etasr.3901.

[11] E. O. Yapıcı, E. Ayli, and O. Nsaif, "Numerical investigation on the performance of a small scale solar chimney power plant for different geometrical parameters," *Journal of Cleaner Production*, vol. 276, Dec. 2020, Art. no. 122908, https://doi.org/10.1016/j.jclepro.2020.122908.

[12] E. Cuce, H. Sena, and P. M. Cuce, "Numerical performance modeling of solar chimney power plants: Influence of chimney height for a pilot plant in Manzanares, Spain," *Sustainable Energy Technologies and*

Assessments, vol. 39, Jun. 2020, Art. no. 100704, https://doi.org/10.1016/j.seta.2020.100704.

[13] A. Atia, S. Bouabdallah, B. Ghernaout, M. Teggar, and T. Benchatti, "Investigation of various absorber surface shapes for performance improvement of solar chimney power plant," *Applied Thermal Engineering*, vol. 235, Nov. 2023, Art. no. 121395, https://doi.org/10.1016/j.applthermaleng.2023.121395.

[14] D. K. Mandal, N. Biswas, A. Barman, R. Chakraborty, and N. K. Manna, "A novel design of absorber surface of solar chimney power plant (SCPP): Thermal assessment, exergy and regression analysis," *Sustainable Energy Technologies and Assessments*, vol. 56, Mar. 2023, Art. no. 103039, https://doi.org/10.1016/j.seta.2023.103039.

[15] S. Hu, D. Y. C. Leung, and J. C. Y. Chan, "Impact of the geometry of divergent chimneys on the power output of a solar chimney power plant," *Energy*, vol. 120, pp. 1-11, Feb. 2017, http://doi.org/10.1016/j.energy.2016.12.098.

[16] D. K. Mandal, N. Biswas, N. K. Manna, and A. C. Benim, "Impact of chimney divergence and sloped absorber on energy efficacy of a solar chimney power plant (SCPP)," *Ain Shams Engineering Journal*, vol. 15, no 2, Feb. 2024, Art. no. 102390, https://doi.org/10.1016/j.asej.2023.102390.

[17] N. Nnabuihe *et al.*, "Preliminary Experimental Performance Study of Hybrid Solar Thermal Collector Coated with Spectrally Selective Polyethylene Terephthalate Film," *International Journal of Advanced Science and Engineering*, vol. 8, no. 4, pp. 2360-2370, 2022, https://doi.org/10.29294/IJASE.8.4.2022.2360-2370.

[18] B. A. Dwiyantoro and S.-W. Chau, "The Influence of Cross-Sectional Shape and Orientation of Micropillar Surface on Microdroplet Formation by a Dewetting Process," *Journal of Engineering and Technological Sciences*, vol. 45, no. 2, pp. 166–178, Jul. 2013, https://doi.org/10.5614/j.eng.technol.sci.2013.45.2.5.

[19] H. Nasraoui, Z. Driss, A. Ayadi, A. Bouabidi, and H. Kchaou, "Numerical and experimental study of the impact of conical chimney angle on the thermodynamic characteristics of a solar chimney power plant," *Proceedings of the Institution of Mechanical Engineers, Part E: Journal of Process Mechanical Engineering*, vol. 233, no. 5, pp. 1185–1199, Oct. 2019, https://doi.org/10.1177/0954408919859160.

[20] S. Dehghani and A. H. Mohammadi, "Optimum dimension of geometric parameters of solar chimney power plants–A multi-objective optimization approach," *Solar Energy*, vol. 105, pp. 603–612, Jul. 2014, https://doi.org/10.1016/j.solener.2014.04.006.

[21] N. Biswas, D. K. Mandal, N. K. Manna, and A. C. Benim, "Novel stair-shaped ground absorber for performance enhancement of solar chimney power plant," Applied Thermal Engineering, vol. 227, Jun. 2023, Art. no. 120466, https://doi.org/10.1016/j.applthermaleng.2023.120466.